A Method for Automatic Extraction of Dopaminergic Neuron Terminals on Striatum Frontal Section Images *

I. Gurevich[1], I. Koryabkina[1], E. Kozina[2], A. Myagkov[3], H. Niemann[4]
M. Ugrumov[2] and V. Yashina[1]

[1] Dorodnicyn Computing Centre of the Russian Academy of Sciences
Vavilov st. 40, 119333 Moscow, Russian Federation

[2] Koltzov Institute of Developmental Biology of the Russian Academy of Sciences
Vavilov st. 40, 119334 Moscow, Russian Federation

[3] Lomonosov Moscow State University
Leninskie Gory GSP-1, 119992 Moscow, Russian Federation

[4] Friedrich-Alexander University of Erlangen-Nuremberg
Martensstr. 3, Erlangen, 91058, Germany

Abstract. This work is devoted to the description of an experimental data acquisition automated method which is required to fill the model of Parkinson's disease preclinical stage. Digital images of the immunostained brain sections of experimental animals are used as a data source. Proposed method: 1) is based on following mathematical morphology operations: opening, grayscale reconstruction, closing, bot-hat transformation, morphological gradient, watershed transformation; 2) enables: to smooth heterogeneous complex background; to select small objects on images depended on given sizes and gray values; to eliminate out-of-focus objects; to separate close objects; to calculate features of selected objects; 3) is intended for automatic extraction of dopaminergic neurons terminals on striatum frontal section images. Experimental investigations confirmed possibility and suitability of section images automated processing and analysis by means of the method. The results of the method use are segmented object contours binary image and object feature list.

1 Introduction

Now and in foreseeable future an image is one of the main tools to represent information in scientific researches, particularly in medicine and biology. Development and application of modern mathematical apparatus for automation of image mining is one of the breakthrough challenges for theoretical computer science. Paper authors developed theoretical basis [1] and elements of information technology [2] for automated morphological image analysis of lymphoid cell nuclei of diseased hemoblastoses, which

* This work was partially supported by the Russian Foundation for Basic Research Grants Nos. 07-07-13545, 08-01-90022 and by the project of the Program of the Presidium of the Russian Academy of Sciences "Fundamental Sciences to Medicine 2009".

Gurevich I., Koryabkina I., Kozina E., Myagkov A., Niemann H., Ugrumov M. and Yashina V. (2009).
A Method for Automatic Extraction of Dopaminergic Neuron Terminals on Striatum Frontal Section Images.
In *Proceedings of the 2nd International Workshop on Image Mining Theory and Applications*, pages 30-39
DOI: 10.5220/0001964600300039

were fundamentals for creation of system for automated diagnostics of blood oncological diseases. This paper is devoted to development of mathematical tools and elements of information technology for analysis of another class of medical images. A current task is automation of experimental data extraction for filling a model of Parkinson's disease (PD) preclinical stage [3].

The disease is characterized by a progressive degeneration of dopaminergic (DA-ergic) neurons [4] in the substantia nigra pars compacta (SN) leading to a dopamine (DA) depletion in the striatum. As a result, parkinsonian patients loose the ability to control their movements. Experimental models' creation is one of the crucial approach to this neurodegenerative disease pathogenesis research.

The development of PD preclinical stage model is a complex screening analysis which is being done cooperatively by physiologists, biochemists and morphologists. The morphological research requires processing and analysis of large quantity of experimental animal serial brain section images. And studying of each of the sections requires quantitative and qualitative feature measurements and analysis of several thousand neurons and axons.

Automatic extraction of dopaminergic neuron terminals on striatum frontal section images allows one to speed up significantly the research of PD at the cost of automatization of experimental data model filling and automatization of model investigation by means of computer experiments.

The initial data is digital images of the immunostained sections of various brain areas. DA-ergic neurons were labeled on serial sections (a thickness is 20 microns) of the substantia nigra (Fig. 1), and their axons (terminals) on sections of the striatum (a thickness is 12 microns) (Fig. 2) by immunohystochemestry for tyrosinehydroxylase (TH). Experimental data have been received from digital images of distal parts of axons (terminals).

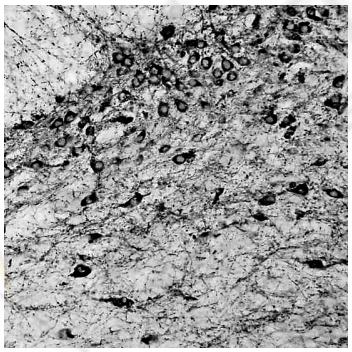

Fig. 1. Neurons.

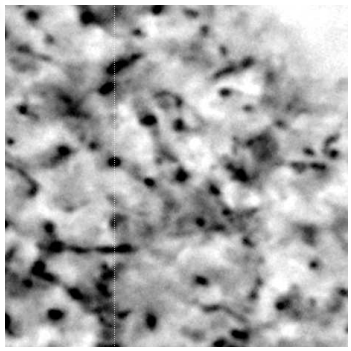

Fig. 2. Terminals.

The major characteristic of PD model is the number of DA-ergic axons, which innervate the striatum. A number of DA-ergic striatum fibers can variate when various schemes of specific dopaminergic neurotoxin – 1-methyl-4phenyl-1,2,3,6-tetrahydropyridine (MPTP) administration (a dose, quantity of injections, intervals between injections) are

used. The extent of degeneration is defined as a difference between the number of terminals of DA-ergic axons in control (the group of animals that were not injected by the toxin) and in experimental (the group of animals that were injected by the toxin) groups. DA-ergic neurons and axons remained after MPTP administration are supposed to have to increase its functional activity to compensate DA deficiency. One of the indicators of increased functional activity of neurons and their fibers is their size increases (hypertrophy). TH – DA synthesis key enzyme – concentration increase can be another specific indicator of functional activity of DA-ergic axons and neurons.

Application of the developed method allows one to quantitatively estimate features mentioned above. The description of the method is given below in Sec. 2. Section 3 reviews the results of the method application.

2 Method Description

The proposed method is designed for the isolation of the small informative elongated objects on the frontal striatum section images and for extracted objects' feature calculation. Images and objects represented on that images were characterized as follows: a) initial image resolution is $0.0117\,\mu\text{m}^2/\text{pixel}^2$; b) terminals (Fig. 2) are rounded objects with area varying from $0.6 - 0.7\,\mu\text{m}^2$ up to $2.5 - 3\,\mu\text{m}^2$; c) terminals color differs from background color; d) terminals can have oval, round, prolate or irregular shape. The results of the method application are segmented object contours binary image and their feature list. The automated segmentation method include 7 stages defined below.

The method stage description is outlined according to the following scheme: 1) brief description of the applied transformation or algorithm and its mathematical content; 2) the significance of the particular transformation while task solving; 3) explanatory material permitting results evaluation. Some method stages are supplied by plots of intensity function for a particular column, which is marked on the corresponding image with thin white dashed line. Intensity function corresponding to particular stage resulting image is plotted with solid line, this of previous stage resulting image (if any) is depicted by dashed line and dash-dot line is used to demonstrate the partial result while applying the transformation. In the equations presented below the grayscale reconstruction [5] of I from marker J is denoted by $\rho_I(J)$ (similar the dual reconstruction [5] is denoted by $\rho_I^*(J)$).

2.1 Step 1. Opening by Reconstruction

Grayscale opening by reconstruction [5, 6], denoted by $I \circ_\rho B$, consists of the following: an initial image I is eroded [6] by a flat structuring element B , then the obtained image $I \ominus B$ is used as marker to reconstruct the initial image.

$$I \circ_\rho B = \rho_I(I \ominus B) \ . \tag{1}$$

The first method step is intended for elimination of initial image narrow peaks, corresponding to the background. The results of carrying out the present transformation are depicted on Fig. 3 and Fig. 4. The erosion was done by the flat disk structuring

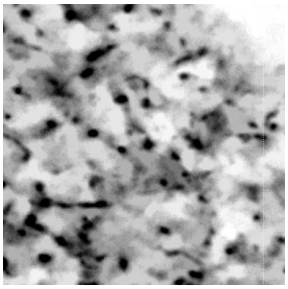

Fig. 3. Opening by Reconstruction.

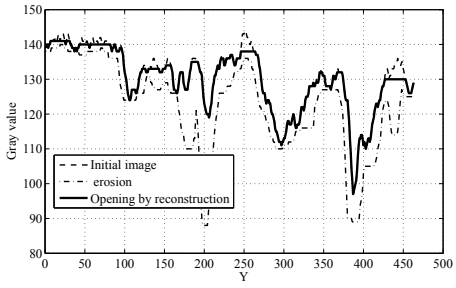

Fig. 4. Opening by Reconstruction. Plot of intensity function. $X = 453$.

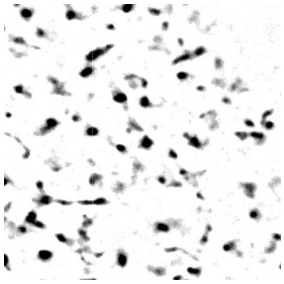

Fig. 5. Bot-Hat by Dual Reconstruction.

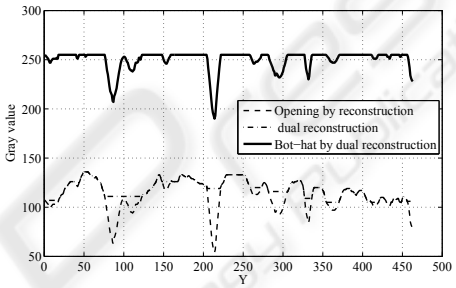

Fig. 6. Bot-Hat by Dual Reconstruction. Plot of intensity function. $X = 149$.

element with the radius that is greater than the narrowest terminal width and that is smaller than the most prolate terminal length.

This step is essential for the reduction of the background regions. There are lots of intensity local minima in these regions, that are used as markers of the objects in the next.

2.2 Step 2. Bot-Hat Transformation by Dual Reconstruction

Grayscale bot-hat transformation by dual reconstruction [5, 7] is the subtraction of the input image from closed by dual reconstruction image (see Sec. 2.3).

$$BotHat_{\rho}^{B}(I) = \rho_{I}^{*}(I \oplus B) - I \ . \tag{2}$$

The main goal of this step is the correction of complex heterogeneous background of the initial image. Figures 5 and 6 reveals the results of bot-hat by dual reconstruction using.

While applying this transformation the inner structure of terminals remains unchanged. It is achieved by using of the dual reconstruction and by the fact, that the used structuring element is grater than almost all terminals.

2.3 Step 3. Closing by Dual Reconstruction

Grayscale closing by dual reconstruction [5, 6], denoted by $I \bullet_\rho B$, consists of the following: an initial image I is dilated [6] by a flat structuring element B, after that the obtained image $I \oplus B$ is used as marker to reconstruct the initial image.

$$I \bullet_\rho B = \rho_I^*(I \oplus B) \ . \tag{3}$$

This step of the method is aimed to nonuniform regions smoothing in the interior of the terminals. The results of carrying out of the present transformation are shown on Fig. 7 and Fig. 8. The structuring element was chosen to be completely contained in all possible terminals.

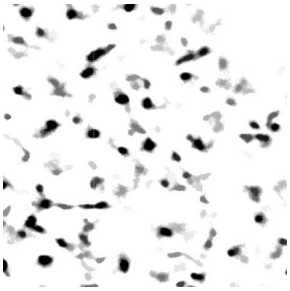

Fig. 7. Closing by Dual Reconstruction.

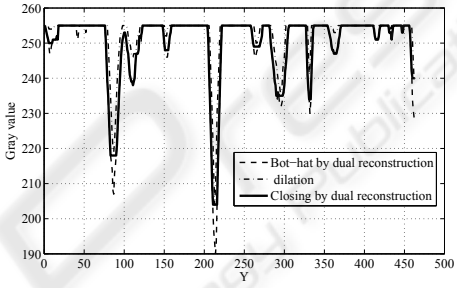

Fig. 8. Closing by Dual Reconstruction. Plot of intensity function. $X = 149$.

This step is essential for providing robust marking of terminals procedure. Whereas, terminal initially have many intensity local minima, the marker extraction procedure will not give appropriate results without the use of current operation.

2.4 Step 4. *H*-dome Elimination Transformation

Reconstruction proved to be a very efficient technique to extract regional maxima and minima from grayscale images. Moreover, the method extends to the determination of such "maximal structures", which are called *h*-domes and *h*-basins [5]. As it was shown in [5] the binary image (mask) $M(I)$ of the regional maxima of I is given by:

$$M(I) = I - \rho_I(I - 1) \ . \tag{4}$$

Then, the *h*-dome $D_h(I)$ image of the *h*-domes of a grayscale image I was defined as follows:

$$D_h(I) = I - \rho_I(I - h) \ . \tag{5}$$

And consequently *h*-dome elimination is the subtraction of an *h*-dome image from the initial image.

Terminals are located at different depth on 12 microns thickness section of the striatum. While taking photos of a section the only section plane is in the microscope focus,

some terminals can have intensity values greater than the others. In addition, sections can be non-uniformly stained, that also involves differences in terminal intensity values. But at first, it is necessary to detect in- and out-of-focus objects. The image with eliminated *h*-domes is presented on Fig. 9 and Fig. 10.

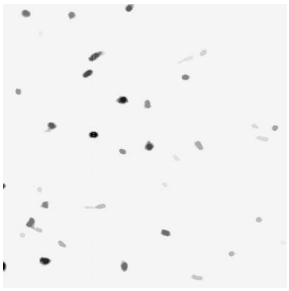

Fig. 9. H-dome elimination.

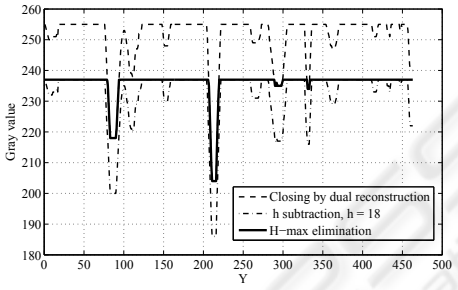

Fig. 10. H-dome elimination. Plot of intensity function. $X = 149$.

A technique for h-parameter estimation was offered for automation of the segmentation procedure. It proceeds on the idea of the selected marker intensity values clustering into two groups. As a result of previous transformations, maxima of all remained objects became equalized, and the focus closeness can be measured by minimal intensity values of the objects which are revealed as regional minima. The initial values for clusters' centers is assigned with minimum and maximum intensity values of the previous step resulting image. To sum up, *h*-dome elimination corresponds to out-of-focus objects removal. H-parameter estimation technique agrees with hand-selected in-focus objects.

2.5 Step 5. Object and Background Markers Extraction

All the previous steps were intended to avoid oversegmentation when applying watershed transformation to morphological gradient image (see Sec. 2.7). Another very effective way to reduce oversegmentation is based on the idea of markers [7, 8]. Object markers are extracted as regional minima of the previous stage resulting image. Background markers are estimated from the distance transform [8] of object markers' binary image. Applying the watershed segmentation algorithm to the modified gradient (see the next step), only marked objects are selected.

2.6 Step 6. Morphological Gradient Image Modification

After marker extraction, grayscale reconstruction is used to modify the gradient image G into an image G' [5] so that:

– its only minima are located on the extracted markers,

– its watershed lines separating markers are preserved.

Figures 11 and 12 represent the morphological gradient image and modified gradient image respectively.

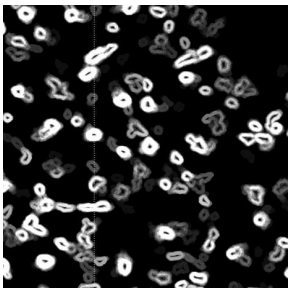

Fig. 11. Morphological Gradient.

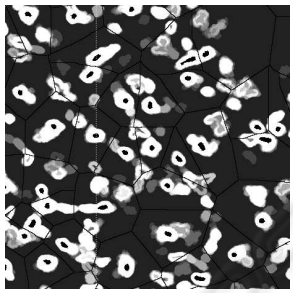

Fig. 12. Modification of Gradient Image.

Morphological gradient image, denoted by G, is obtained as the difference between the dilation and the erosion of the Step 3 (Sec. 2.3) resulting image by the same structuring element.

$$G(p,q) = (I \oplus B)(p,q) - (I \ominus B)(p,q) \ . \tag{6}$$

Then the binary marker image M, revealed at the previous step, is used to modify G in the following way:

$$G' = \rho^*_{\min(G+1,(m+1)M)}((m+1)M) \ , \tag{7}$$

where m is the maximal value of the pixels of G.

2.7 Step 7. Watershed Segmentation

On this step the modified gradient is processed with watershed segmentation algorithm [8, 9], and, as a result, object contours are retrieved. Figures 13 and 14 reveals the modified gradient and watersheds lines intensity function plots.

3 Experimental Check of Proposed Method

The initial image with white color marked object boundaries, revealed during the proposed method application, is presented at Fig. 15. Figure 16 depicts manually extracted objects for the same image.

With the aid of the developed method ten striatum frontal section images (five belong to experimental group and five – to control group) were analyzed. Main subtasks of this analysis were the following: automated and manual extracted objects comparison; terminal features calculation; experimental and control groups differences detection. Following data was found for each image and for each group of images: 1. selected

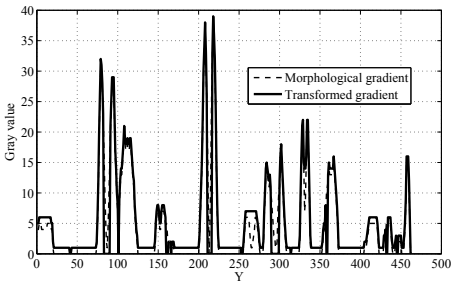

Fig. 13. Modified gradient. Plot of intensity function. $X = 149$.

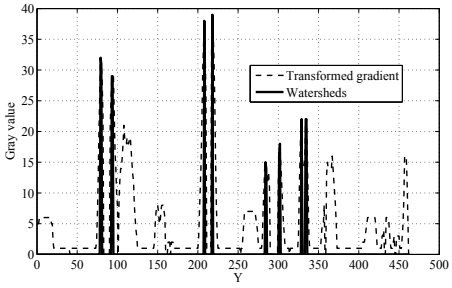

Fig. 14. Watersheds of modified gradient. Plot of intensity function. $X = 149$.

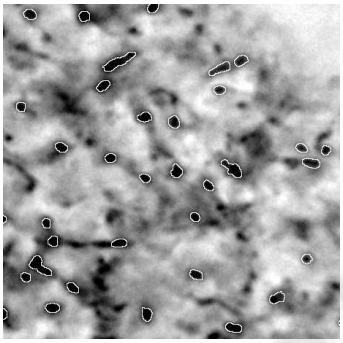

Fig. 15. Automatic extraction.

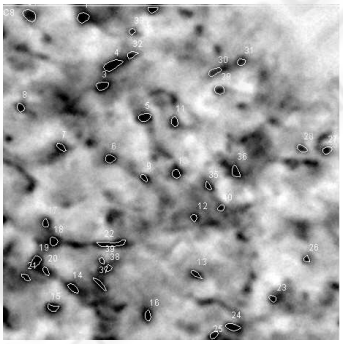

Fig. 16. Manual extraction.

objects' numeric features (perimeter; area; minimum, mean and maximum of intensity values; shape factor); 2. averaged numeric features; 3. results of hypothesis tests to compare the distributions of feature values in manual and automated calculations; 4. correlation analysis 5. explanatory material permitting manual and automated selected object areas and mean gray values comparison: (a) plots for comparison and evaluation of area distribution fractiles; (b) plots for comparison and evaluation of mean value distribution fractiles; (c) plots of joint area and mean gray value distribution.

Table 1 contains means and standard deviations of terminal area and mean gray value distributions, when different ways of object selection techniques are used. In this table coincident objects are those, that were the same while extracting them manually and automatically

Such a considerable difference in the mean area becomes clear if we take into account the fact that the human vision is not so perfect in detecting precise boundaries of the objects and the fact that morphologists extract not all objects presented on an image, but only those they believe to be in-focus terminals. Furthermore the manual terminal extraction was done with computer mouse and it is not always possible to control hand and mouse movements totally. But, in spite of all written above the hypothesis tests allow us to conclude that there is no reliable difference between area distribu-

Table 1. Area and mean gray value distribution average characteristics in “experiment” and “control”.

Average characteristic	Estimation method	Area		Mean gray value	
		experiment	control	experiment	control
Mean	manual estimation	1.372	1.303	96.227	82.927
	coincident objects	1.555	1.700	95.789	83.596
	automated estimation	1.749	1.731	100.677	88.614
Standard deviation	manual estimation	0.692	0.520	9.928	10.766
	coincident objects	0.562	0.695	10.982	11.569
	automated estimation	0.694	0.705	12.245	14.705

tions in manual and automated estimation. The results also were satisfactory for PD experts. Concerning a little difference in manually estimated area it can be guessed that the method extracts more essential objects. Hypothesis tests on area distributions give the following results: there is no reliable difference between control and experimental groups in manual estimation and there is such a difference in automated estimation.

The number of objects extracted manually and automatically on the initial image fragment and automatically on the whole image are given in Tab. 2, where in image names “c” stands for control and “e” – for experiment.

Table 2. Terminals number.

Image	1–c	2–e	3–c	4–e	5–c	6–e	7–c	8–e	9–c	10–e
Automatic segmentation (whole)	1664	900	1623	891	1423	917	1632	899	1980	1002
Manual extraction (fragment)	40	11	29	20	36	14	35	11	33	12
Automatic segmentation (fragment)	36	16	34	20	35	15	43	12	34	13

4 Conclusions

Experimental investigations confirmed the possibility and the suitability of immunostained striatum frontal section images automated processing and analysis by means of developed method and with the aim to define characteristics, which are essential for preclinical stage PD model construction. The designed method for automatic extraction and feature calculation of dopaminergic neurons terminals on section images is also established to allow obtaining the results with precision comparable those of manual object feature estimation. The same methods can be developed for similar problems solving.

Experiments revealed following: 1) considerable decrease in terminal numbers of DA-ergic axons in experimental group in comparison to terminal numbers in control group; 2) change in DA-ergic neuron functional activity after neurotoxin administration. The obtained results are the important stage of a condition of dopaminergic nigrostriatal system estimation researches at developing PD. Hereafter it will allow of compensatory mechanisms research.

In the future selected object clustering in an extended feature space is planned. It is aimed to statement and solving a problem of automatically extracted objects assignment to selected clusters.

References

1. Gurevich, I.B., Yashina, V.V., Koryabkina, I.V., Niemann, H., Salvetti, O.: Descriptive approach to medical image mining: An algorithmic scheme for analysis of cytological specimens. Pattern Recognition and Image Analysis: Advances in Mathematical Theory and Applications 18 (2008) 542–562
2. Gurevich, I., Harazishvili, D., Jernova, I., et al.: Information technology for the morphological analysis of the lymphoid cell nuclei. In: The 13th Scandinavian Conference on Image Analysis. Volume 2749 of LNCS. (2003) 541–548
3. Albin, R.L., Young, A.B., Penney, J.B.: The functional anatomy of basal ganglia disorders. Trends Neurosci 12 (1989) 366–75
4. Tipton, K.F., Singer, T.P.: Advances in our understanding of the mechanisms of the neurotoxicity of mptp and related compounds. J Neurochem 61 (1993) 1191–1206
5. Vincent, L.: Morphological grayscale reconstruction in image analysis: Applications and efficient algorithms. IEEE Transactions on Image Processing 2 (1993) 176–201
6. Soille, P.: Morphological Image Analysis: Principles and Applications. Springer, Berlin (2004)
7. Wu, Q., Merchant, F., Castleman, K.: MICROSCOPE IMAGE PROCESSING. Elsevier Inc. (2008)
8. Gonsales, R.C., Woods, R.E.: Digital Image Processing. 2 edn. Pearson Education, Inc (2002) publishing as Prentice Hall.
9. Vincent, L., Soille, P.: Watersheds in digital spaces: an efficient algorithm based on immersion simulations. IEEE Trans. Pattern Anal. Machine Intell. 6 (1991) 583–598